Tribological Behavior of Hybrid AA6061/SiC/Carbonized Coconut Shell Nanocomposites

Abstract

In the present investigation, hybrid aluminum matrix composite was prepared by stir casting method using aluminum alloy 6061 as the matrix material and nanoparticles of carbonized coconut shell (CCS) and silicon carbide (SiC) as reinforcements, and characterized for wear behavior. The average reinforcement particle sizes were 42.3 nm and 50.01 nm for SiC and CCS respectively. The weight percentage of CCS and SiC nanoparticles were varied at equal amounts ranging from 3 to 15 wt.%, with 3 wt.% steps. Wear test was done on a Pin on disc apparatus at varying load of 10 N, 20 N, 30 N, 40 N and 50 N under dry sliding conditions, at a constant speed of 2.0 m/s and a sliding distance of 400 mm. The wear loss and wear rate of each sample during the wear process was recorded by using a computer. The chemical composition and microstructural study of the composites were done using x-ray fluorescence (XRF) and scanning electron microscope (SEM), which revealed uniform distribution of nanoparticles of CCS (containing majorly SiO_2, Al_2O_3 and Fe_2O_3) and SiC in the matrix alloy. The wear results revealed that both the volumetric wear loss and wear rate of the composites decreased with increased weight percent of reinforcement, but increased with increased load. The results also indicated that the coefficient of friction of the composites increased with increased weight percent of reinforcement, particle size and applied loads.

Keywords: Aluminum; stir casting, wear behavior; wear rate; nanoparticles.

Introduction

Aluminum-based matrix composites (AMCs) are very attractive for lightweight applications such as automobile, aerospace, military and transport sectors due to high specific strength, low density, durability, machinability, availability, cost effectiveness, good fatigue properties and wear resistance [1, 2]. In addition, AMCs offer the possibility to tailor their properties to meet specific requirements [1]. This could include increased strength, decreased weight, higher service temperature, improved wear resistance, higher elastic modulus, controlled coefficient of thermal expansion, improved fatigue properties, etc. [3-5].

The property of the AMCs depends on the property of the matrix and the reinforcement. The addition of reinforcements into the metallic matrix improves the stiffness, specific strength, wear, creep and fatigue properties compared to the conventional engineering materials [6]. The reinforcement in AMCs may be in the structure of continuous fibres, discontinuous fibres, whiskers or particulates with volume fractions ranging from a few percent (about 15 vol%) to 70 vol%. Ceramic materials being used as reinforcement in AMCs consists of silicon carbides (SiC), titanium borides (TiB_2), alumina (Al_2O_3), nitrides, boron and graphite. Recently, reinforcements commonly used in aluminium matrix composites have been extended to include agro-wastes such as rice waste ash, palm oil fuel ash, sugar cane bagasse, palm karnel ash, periwinkle shell ash and coconut shell ash [7, 8]. These agro-wastes are cheap and readily available in high quantity.

In this work, an attempt has been made to prepare hybrid aluminium matrix composites (HAMC) by adding carbonized coconut nanoparticles and SiC reinforcement particles into AA6061 matrix alloy using a stir casting method. The carbonized coconut nanoparticles and SiC reinforcement particles weight percentage were varied at equal amounts. The objective of the present investigation is to determine the wear properties of the HAMC by adding hard ceramic particles into the aluminium alloy.

Materials and Method

The materials used in this study include aluminium alloy 6061 (base alloy), silicon carbide and carbonized coconut shell (reinforcements). Table 1 shows the chemical composition of AA6061 alloy. Samples of the hybrid composites consisting of carbonized coconut shell particles CCS and silicon carbides SiC were fabricated using stir casting method (Figure 1). The reinforcements with average particle sizes of 42.3 nm and 50.01 nm for SiC and CCS respectively were used for producing different samples of the composite containing 3, 6, 9, 12 and 15 wt% each of CCS and SiC. The stir casting process started with placing the empty crucible in the furnace. The base alloy and was melted at 700 ºC in a crucible. Simultaneously reinforcements were preheated to a temperature of 300 ºC to remove moisture, enhance wettability and reduce the temperature gradient between molten metal and reinforcements. Magnesium of 1 wt.% was then added to the molten metal to enhance the wettability between reinforcements and molten metal [9, 10].

Figure 1: Preparation of samples: (a) Coconut shells (b) Silicon carbide (c) CCS (d) Furnace (e) Molding process (f) Cast samples

Table 1: Composition of AA6061.

Element	Si	Fe	Cu	Mn	Mg	Ni	Zn	Ti	Cr	Al
Weight %	0.514	0.230	0.161	0.071	0.960	0.010	0.015	0.031	0.103	Bal.

Chemical Composition of Reinforcement Particulates

Mini Pal compact energy dispersive X-ray fluorescence machine was used for chemical compositional and elemental analysis of particulates of carbonized coconut shell. The system is controlled by a computer running the Mini Pal analytical software.

Wear Testing

Wear measurement was carried out to determine the amount of materials removed (or worn away) after a wear test, (and in reality after a part in service for a period of time). The material worn away can be expressed either as weight (mass) loss, volume loss, or linear dimension change depending on the purpose of the test, the type of wear, the geometry and size of the test specimens and sometimes on the availability

of a measurement facility. Dry sliding wear tests for different specimens were conducted in pin on disc tester of DUCOM make (Figure 2).

Figure 2: Wear test setup

The test specimens were AA6061 alloy with 0, 3, 6, 9, 12 and 15 % reinforcements (equal weight percentage of both carbonized coconut shell particles and silicon carbide particles). The specimens for wear test were prepared based on ASTM standard. The diameter of pin specimen prepared was 12 mm. The sliding distance was taken constant as 400 m and the variable parameters were load of 10, 20, 30, 40, 50 N, at a constant sliding velocity of 2.0 m/s. From the sliding velocity, the speed of disc is calculated using the formula:

$$\text{Rotating speed of disc (rpm)} = \frac{60 \times V}{\pi \times D} \quad (1)$$

where V is the sliding velocity in m/s and D the track diameter in meters (m).
The rotation time of disc is set and is calculated by using sliding distance.

$$\text{Rotating time (seconds)} = \frac{Distance}{Sliding\ velocity} \quad (2)$$

The surfaces of pin samples were prepared using an emery paper prior to test in order to ensure smooth surface contact with steel disc before start of each experiment. Also, the wear track was cleaned with an emery paper and then with acetone in order to remove the specimen traces which is adhered to disc track. Before the start of experiment, the pin was weighed and it was held in the specimen holder against the counter face rotating disc (steel disc) with wear track diameter of 80 mm. The pin was loaded against the disc through dead weights on the lever. The load cell on this lever arm helps determine the wear at any point of time by monitoring the movement of the arm. When disc is rotated, the load cell which is connected to the computer receives the signal and the friction force is recorded. The wear disc was then allowed to rotate at a calculated speed (rpm) and time according to velocity. After each experiment, the weight was measured and the loss of weight was calculated. The same procedure was repeated for all the experiments and wear rate was calculated for each pin using Equation 3.

$$\text{Wear rate (mm}^3\text{/m)} = \frac{\delta m}{\rho \times d} \quad (3)$$

where δm is difference in mass, ρ is density of the material and d is sliding distance.
To determine the coefficient of friction of the composites, a measuring scale was used to measure the perpendicular forces acting on the sample and the resistive forces by the sample. The varied load from 10 to 50 N at an interval of 10 N were applied to the sample with varied weight of SiC and carbonized coconut shells as reinforcement from 3 to 15 wt% at an interval of 3 wt% and were made to slide on the sliding

platform of the measuring scale. The resistive forces as well as the perpendicular forces were read off from the scale. The coefficient of friction μ, was then calculated using Equation 4 [13].

$$\mu = \frac{F_r}{N} \quad (4)$$

where F_r is the measured friction force and N the normal reaction.

Results and Discussion

Chemical Composition of Reinforcements

The results obtained from the XRF chemical compositional analysis of the carbonized coconut shell particles (CCSp) and SiC shown in Table 2, revealed that the carbonized coconut particulates contained SiO_2, MgO, Al_2O_3 and Fe_2O_3 in great amount with small amounts of CaO, K_2O, Na_2O, MnO and ZnO. The presence of hard substances like SiO_2, Al_2O_3 and Fe_2O_3 suggest that the carbonized coconut shell particles can be used as particulate reinforcement in various metal matrix composites [11, 12]. This result is consistent with the results by Donald *et al.* [14], Apasi *et al.* [11] and Madakson *et al.* [12], and the chemical composition has similarity with the XRF analysis of periwinkle shell ash, rice husk ash, fly ash and bagasse ash currently used in metal matrix composite as reported by Nwabufoh [15], Hassan and Aigbodion [15] and Rajan *et al.* [17]. Therefore, the present work suggests the suitability of carbonized coconut shell as particulates reinforcement in metal matrix composites.

Table 2: Chemical composition of reinforcements.

CCS									
Element	Al_2O_3	CaO	Fe_2O_3	K_2O	MgO	Na_2O	SiO_2	MnO	ZnO
%	16.50	0.58	14.50	0.51	16.51	0.50	46.70	0.42	0.35
SiC									
Element	SiC	Si	SiO_2	Fe	Al	C			
%	98.6	0.30	0.6	0.09	0.10	0.3			

Microstructure of Composites

The SEM micrographs of the AA6061 alloy and those of the composites are shown in Figure 3. Figure 3(a) shows the micrograph of the unreinforced alloy revealing the white α −phase with equiaxed grain shape [18]. Fine grains are found dissipated along as far as possible in the structure of AA6061 alloy. Notably, the result of SEM for microstructural examination of the specimens shown in Figure 2(b), reveals a fairly uniform distribution of SiC and carbonized coconut particles in the matrix in all %wt addition of the reinforcements. The uniform distribution of SiC and carbonized coconut particles in the matrix can be attributed to a number of factors which includes, effective stirring of the melt, degassing tablet used and good wettability that resulted in improved interfacial bonding between the matrix and the coconut shell ash particles [11]. No segregation of SiC and carbonized coconut particles were found along the grain boundaries. Distribution of particles was observed to be intra-granular, in which the majority of the particles locate inside the grains. This distribution is preferred in AMCs to have better mechanical and tribological properties. Silicon carbide and carbonized coconut particles were thermodynamically stable, and there were no pores or voids around them. The reinforcement particles resisted aluminium grain growth and resulted in nucleation sites growth, which led to the formation of finer grains. As the concentration of SiC and carbonized coconut shell particles increased in the matrix, composite properties

such as hardness and resistance to wear also showed improvement. Figure 3(c) represents the higher magnification (1000×) of the Al6061/15% SiC composite. It indicates that the interface between the matrix and dispersed phase is clear, since any reaction products were not presented.

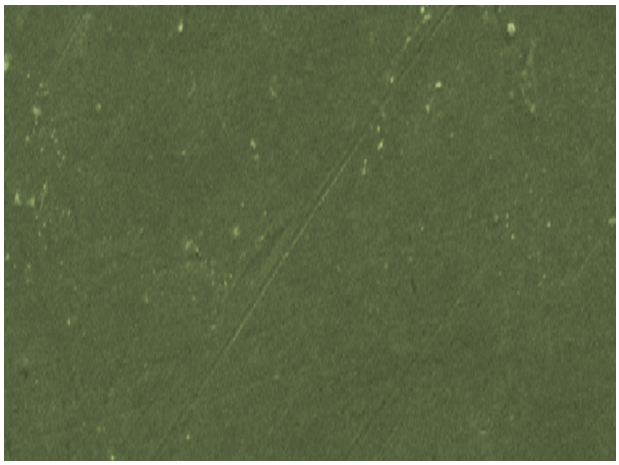

(a) SEM image of AA6061 alloy

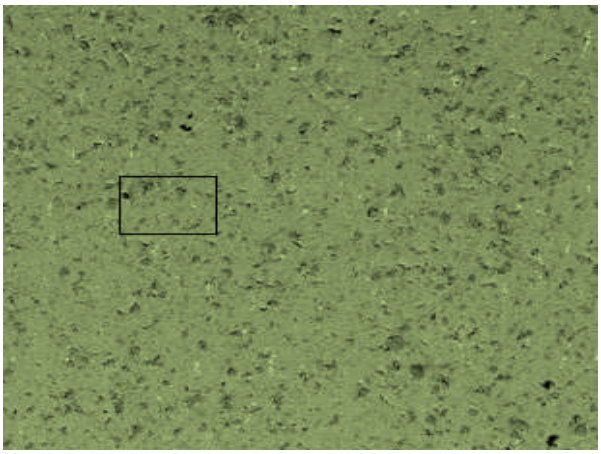

(b) 3 wt.% SiC/CSS

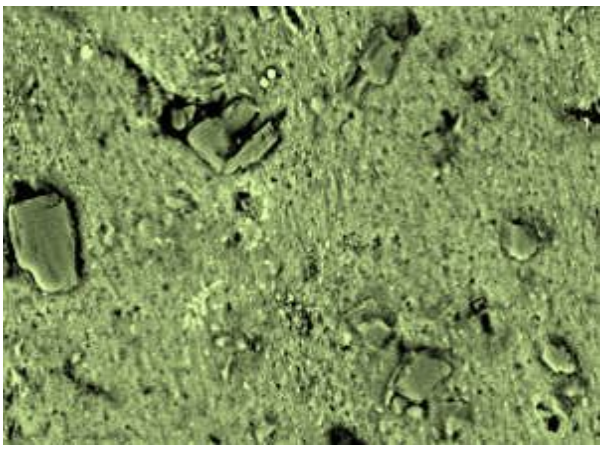

(c) 6 wt.% SiC/CSS

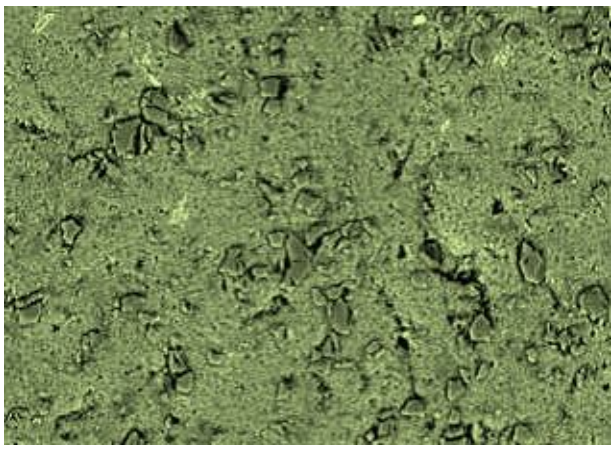

(d) **9 wt.% SiC/CSS**

Figure 3: SEM micrographs of composites

Effect of Content and Particle size on Wear Behavior of Composites

The SEM micrographs of the worn surfaces for the wear test conducted for composite specimens as a function of nCCS/nSiC particulates content at constant load of 50 N at a constant speed of 2.0 m/s and a sliding distance of 400 mm are shown in Figure 4. In the case of aluminium alloy with CCS/SiC reinforcements (Figure 4b), there appeared to be some disruption of the transfer film which affected the wear rate performance. The worn surface of the materials can be described as classical ratcheting wear, as defined by Monikandan *et al*. [19]. The transition in wear rate observed for many MMCs is faster and is believed to be the result of voiding/cracking between the reinforcement and the matrix, both of which led to fragmentation and delimitation of the surface [19].

Figure 4(b) also revealed particle cutting and void formations due to chips of the matrix. There is also evidence of AA6061 alloy removal, and deep furrows in the structure. The propagation of cracks along transverse, as well as longitudinal directions is well visualized. Furthermore, crushed and fragmented particles were noticed. The worn surfaces in some places revealed patches from where the material was removed from the surface of the material. The parallel grooves suggested abrasive wear as characterized by

the penetration of the hard SiC and carbonized coconut shell particles into a softer surface, which is an important contributor to the wear behaviour of AA6061/SiC/CCSp composites. It is possible that the scored grooves might have been formed due to the action of the wear- hardened deposits on the disc track. Similar observations were made by Monikandan *et al*. [19].

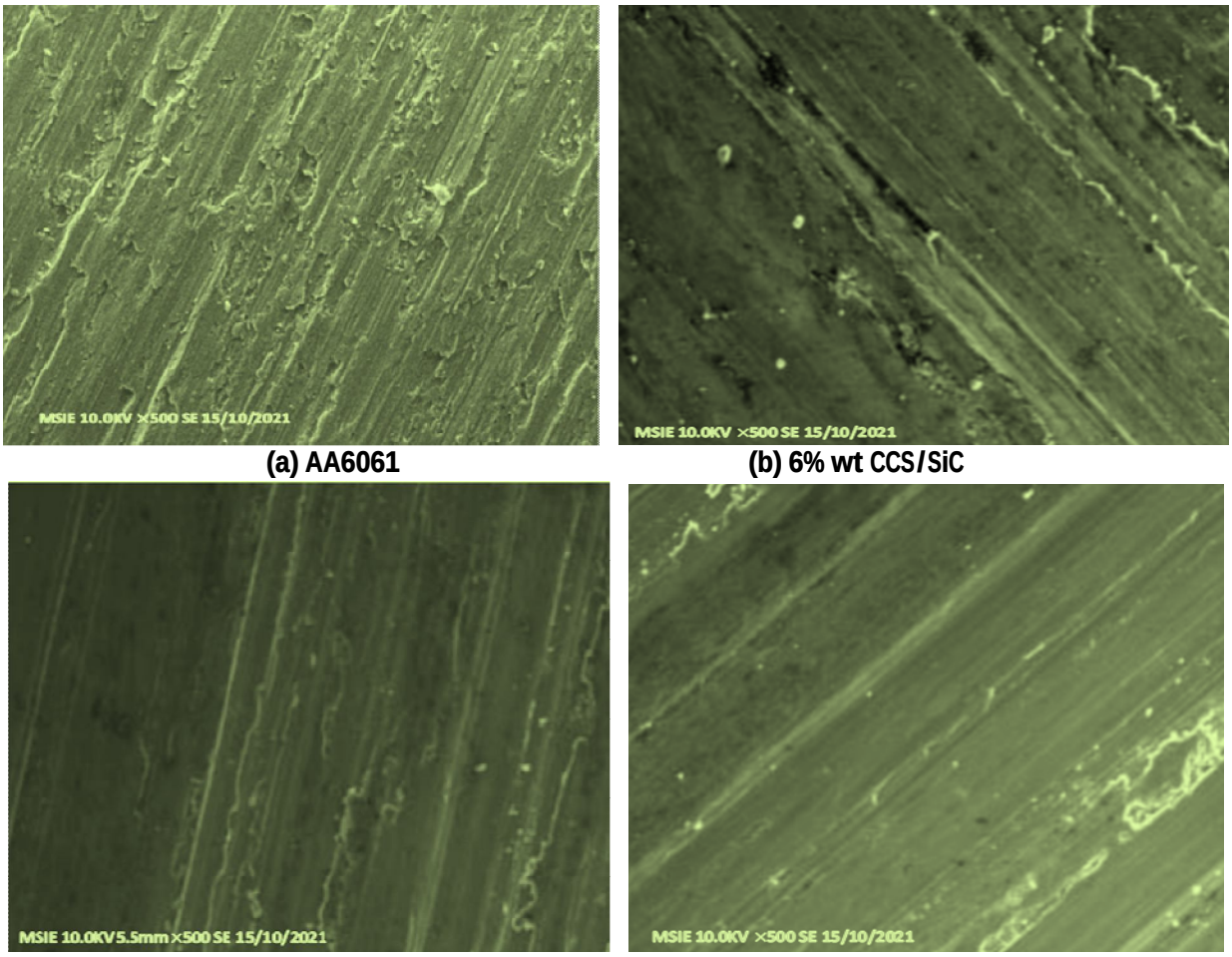

(a) AA6061 (b) 6% wt CCS/SiC

(c) 12% wt CCS/SiC (d) 15% wt CCS/SiC

Figure 4: SEM of the worn surfaces of composites with nSiC/nCCSp at 50 N, 2.0 m/s and 400 mm.

Effect of Applied Load on Wear Behaviour of the Composites

Figure 5 represents the SEM micrographs of the worn surface of Al6061/6 wt.% nCCS/nSiC particulates specimens as a function of applied load. The worn surface appears relatively smooth at a lower load of 10 N. There are no deeper grooves or plastic deformation. The subsurface remains intact. The increase in applied load increased the plastic deformation on the worn surface and the formation of pits. The sub-surface is exposed at a higher load of 50 N. This confirms that the penetration of counterface asperities was more at higher load. The overall wear mode appears to be abrasive. The parallel groove pattern can be seen in all the worn surfaces. Nevertheless, the effect of applied load is well pronounced in the form of plastic deformation at the edge of grooves and existence of pits.

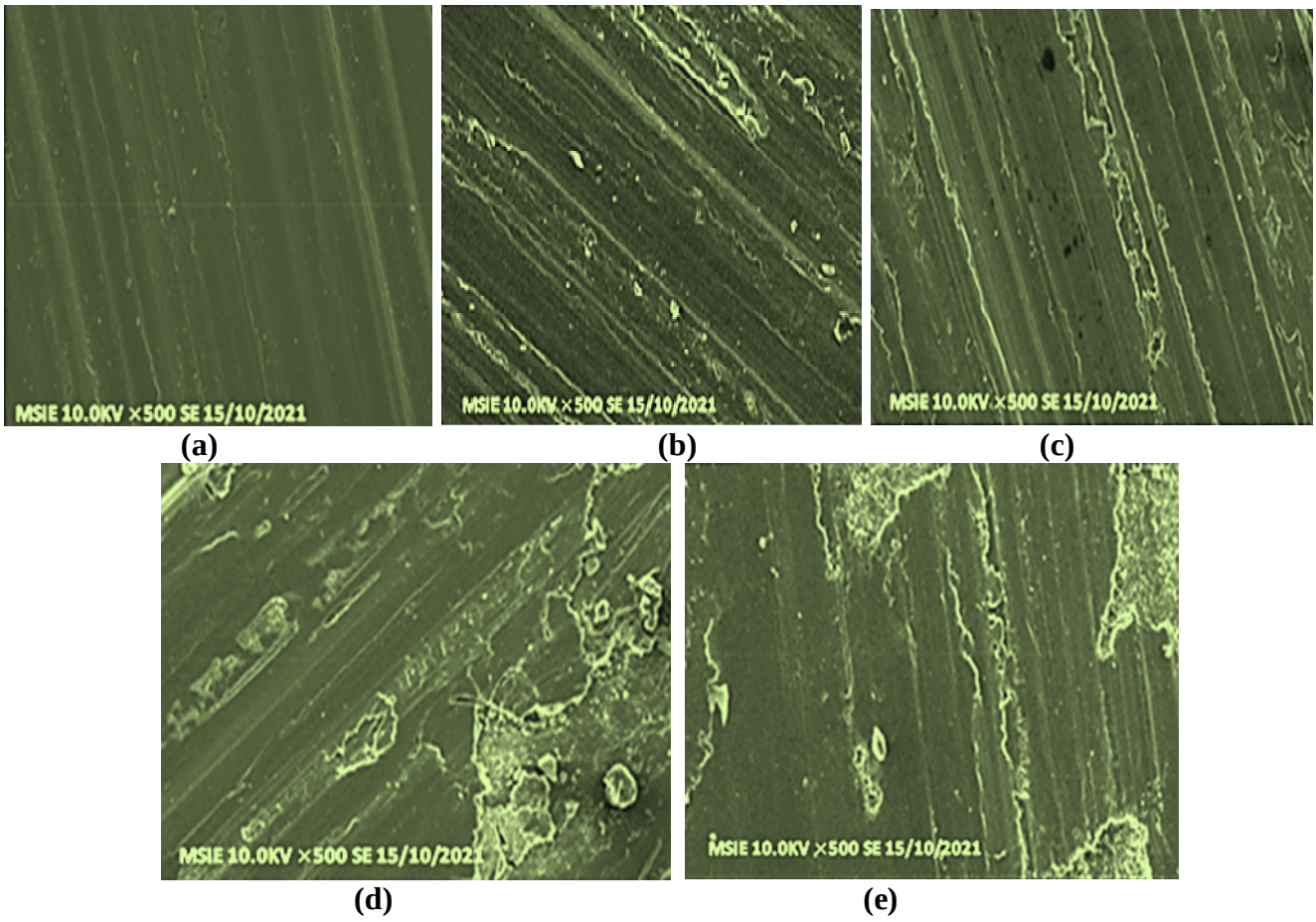

Figure 5: SEM micrographs of worn surface of Al6061/6 wt.% nCCS/nSiC at applied load; (a) 10 N, (b) 20 N, (c) 30 N, (d) 40 N and (e) 50 N..

The results of the wear loss and wear rate are shown in Figure 6 and Table 3. Since the relative size of the reinforcement is small in particulate-reinforced composites, the effect of the interfacial toughness on the wear rate can be significant. For example, when the interface is weak, the reinforcement can be readily removed during abrasive wear conditions, such that a negative reinforcement effect is observed [20]. Indeed, as shown in Table 3, the wear rates in the composite were lower than those in the unreinforced matrix; moreover, with increasing reinforcement volume fraction, the wear rates were further decreased.

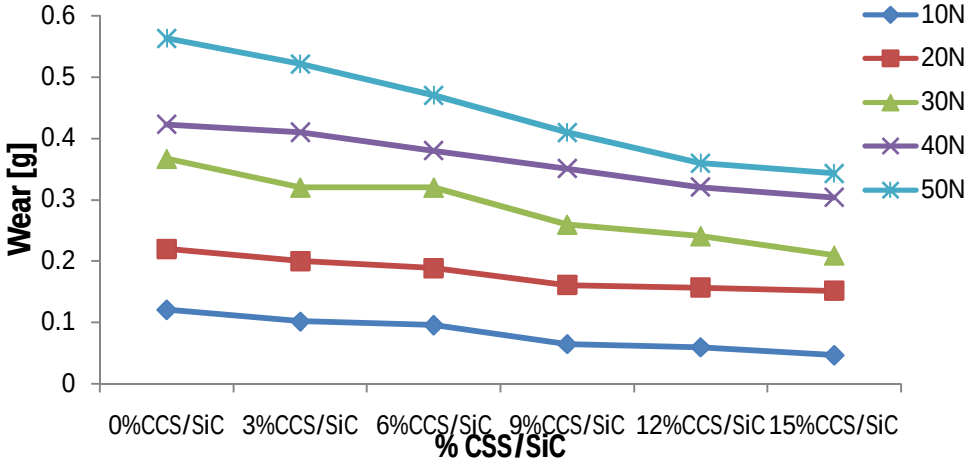

Figure 6: Variation of wear loss with composition of composite

Table 3: Wear rate of the composites (mm^3/m).

S/N	Wt % CCS/SiC	Load [N]				
		10	20	30	40	50
1	0	0.1077	0.1957	0.3265	0.3763	0.5009
2	3	0.0907	0.1786	0.2857	0.3661	0.4652
3	6	0.0873	0.1718	0.2736	0.3455	0.4273
4	9	0.0600	0.1485	0.2399	0.3238	0.3782
5	12	0.0558	0.1459	0.2240	0.2983	0.3346
6	15	0.0452	0.1462	0.14612	0.2923	0.3500

The effect on friction coefficient of AA6061/nCCS/nSiC matrix composite as given in Tables 4 revealed that the coefficient of friction also increased with increasing weight percent of reinforcement, particle size and applied loads. The reason for this trend may be due to increase in the amount of debris from the composites which are also abrasive in nature and since the Al alloy matrix is soft which in turn allow the debris to adhere to the surface of the Al composite resulting in an increase in both friction coefficient and friction force during contact period. The same trends are also reported in Al-Si-Fe-coconut shell ash composites [11], Al-rice husk ash composites [21], Al-bagasse ash composites [22].

Table 4: Coefficient of friction of composites at varying loads with nCCS/nSiC.

S/N	Wt%CCSp/SiC	Load [N]				
		10	20	30	40	50
1	0	0.18	0.23	0.39	0.48	0.54
2	3	0.26	0.33	0.47	0.63	0.71
3	6	0.30	0.38	0.55	0.67	0.75
4	9	0.34	0.42	0.61	0.72	0.80
5	12	0.38	0.44	0.68	0.73	0.84
6	15	0.39	0.47	0.71	0.76	0.86

Wear Rate Model Predictions

Results of regression model developed for AA6061/CCSnp/SiC composites wear rate (W) response, the applied load (P) and weight percent of reinforcement, as the predictor/independent variables are presented in Figure 7 and Table 5. Constancy of speed (2.0 m/s), time (seconds) and sliding distance (400 mm) remains throughout the model development. A good fit of the model with experimental wear rate (response) is established (Figure 7). Equation 4 shows the model function for predicting the response genes at all levels of predictor/independent variable. Evaluation of the model reveals that the model is statistically relevant in explaining the relationship between the wear rate (dependent variable) and independent variable (P). However, the model accounts for 87 % of the experimental data, an indication that little residuals (which are less than 12.5 %) are observed between the theoretical and actual wear rates of AA6061/nSiC/nCCS composites which established a reasonable agreement as required.

$$\text{Wear rate} = \beta_0 + \beta_1(Wt) + \beta_2(P)^n \qquad \text{Equation 4 (a)}$$

With $\beta_0 = 0.05$, $\beta_1 = 0.00775$ $\beta_2 = 0.07415$ and $n = 1$, the model equation becomes

$$\text{Wear rate} = 0.05 + 0.00775(\text{Wt\% CCSp/SiC}) + 0.07415(\text{Load}) \qquad \text{Equation 4 (b)}$$

Table 5: Wear rate.

Wt.% nCCS/nSiC	Load (N)	Experimental Wear Rate (mm^3/m)	Model Predicted Wear Rate (mm^3/m)	Deviation (%)
0	10	0.1077	0.1207	+12.07
3	20	0.1786	0.1954	+ 9.41
6	30	0.2736	0.2487	-9.10
9	40	0.3238	0.2933	-9.42
12	50	0.3346	0.3331	-0.45
15	50	0.3500	0.3564	+1.80

$$\text{Wear rate} = \beta_0 + \beta_1(Wt) + \beta_2(P)^n \qquad \text{Equation 4.4(a)}$$

With $\beta_0 = 0.05$, $\beta_1 = 0.00775$ $\beta_2 = 0.07415$ and $n = 1$, the model equation becomes

$$\text{Wear rate} = 0.05 + 0.00775(\text{Wt\% CCSp/SiC}) + 0.07415(\text{Load}) \qquad \text{Equation 4.4(b)}$$

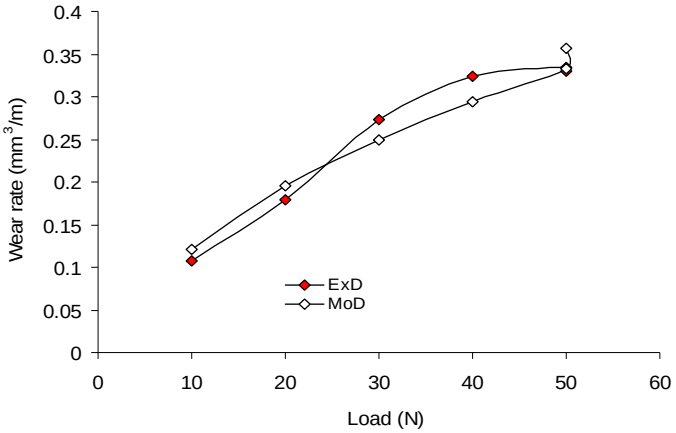

Figure 7: Variation of experimental and model wear rates with loading of composites.

Conclusion

The tribological behavior of hybrid aluminum composite reinforced with equal proportions of nanoparticles of silicon carbide and carbonized coconut shell was successfully investigated with the following findings;

1. Carbonized coconut shell particles contain great amount of hard substances like SiO_2, Al_2O_3 and Fe_2O_3 which in addition to SiC strengthened the soft Al matrix.
2. The microstructure of the composites revealed uniform dispersion of reinforcement particles in the alloy matrix with excellent interfacial bond.
3. The wear rate decreased with increased weight percent of reinforcement, but increased with increased load.
4. The coefficient of friction of the composites increased with increased weight percent of reinforcement, particle size and applied loads.
5. The developed composites could be suitable for applications requiring good wear resistance.

References

1. Wang, Z., Prashanth, K.G., Scudino, S., Chaubey, A.K., Sordelet, D.J., Zhang, W.W., Li, Y.Y. and Eckert, J. Tensile properties of aluminium matrix composites reinforced with in situ $Al_{84}Gd_6Ni_7Co_3$ glassy particles. *Journal of Alloys Compound*, 2014; 86: 419 – 422.
2. Karl, U. K. *Metal Matrix Composites. Custom-made Materials for Automotive and Aerospace Engineering.* WILEY-VCH Verlag GmbH & Co. KGaA, Weinheim, 2006; 820p.
3. Parswajinan, C., Vijaya, B. R., Abishe, B., Niharishsagar, B. and Sridhar, G. *Hardness and impact behaviour of aluminium metal matrix composite*. *The 3rd International Conference on Materials and Manufacturing Engineering. IOP Conference Series: Materials Science and Engineering 390.* 8 – 9 March 2018. Sri Chandrasekharendra Saraswathi Viswa Mahavidyalaya University, Kancheepuram, India, 6p.
4. Sudipt, K. and Ananda T. J. *Production and Characterisation of Aluminium-Fly Ash Composite using Stir Casting Method*. BTech. Project. National Institute of Technology, Rourkela, 2008; 73p.
5. Michael, O. B., Kenneth, K. A. and Lesley, C. Aluminium matrix hybrid composites: A review of reinforcement philosophies; mechanical, corrosion and tribological characteristics. *Journal of Materials Research and Technology*, 2015; 4 (4): 434 – 445.
6. Vijaya, R. B., Elanchezhian, C., Annamalai, R. M., Aravind, Sri Ananda, A. S. T., V. Vignesh, V. and Subramanian, C. Aluminium metal matrix composites - A review. *Review, Advanced Materials Science*, 2014; 38: 55 – 60.
7. Senthilkumar, G., Manoharan, S., Balasubramanian, K. and Dhanasakkaravarthi, B. An experimental investigation of metal matrix composites of aluminium (Lm6), boron carbide and fly ash. *Australian Journal of Basic and Applied Sciences*, 2016; 10 (1): 137 – 144.
8. Iyasele, E. O. Comparative analysis on the mechanical properties of a metal matrix composite reinforced with palm kernel/periwinkle shell ash. *Global Scientific Journal*, 2018; 6 (8): 1 – 24.
9. Nwigbo, M. N., Lasisi, U. E. and Ukaru, N. Y. Comparative study of tensile properties of hybrid AA6061/SiC/carbonized coconut shell micro and nano composites. *International Journal of Mechanical and Civil Engineering*, 2022; 5 (1): 10 – 24.
10. Nwigbo, M. N. and Lasisi, U. E. Applicability of carbonized coconut shell particulates and silicon carbides in synthesis of hybrid aluminium matrix composites. *European Journal of Materials Science*, 2022; 9 (1): 1 – 17.
11. Apasi, A., Yawas, D. S., Abdulkareem, S. and Kolawole, M. Y. Improving mechanical properties of aluminium alloy through addition of coconut shell-ash. *Journal of Science and Technology*, 2016; 36 (3): 34-43.
12. Madakson, P. B., Aigbondon, V. S., Apasi, and Yawas, D. S. Wear behaviour of AlSi-Fe alloy/coconut shell ash particulate composites. *Tribology in industry*, 2012; 34 (1): 36 - 43.
13. Bello, S. A., Agunsoye J. O., Adebisi J. A., Kolawole F. O. and Hassan S. B. Physical properties of coconut shell nanoparticles. *University Journal of Science, Engineering and Technology*, 2016; 12 (1): 63-79.
14. Donald, A.O., Hassan, M.A., Hamza, S., Garba, E., Dangtim, D.K. and Mamadou, M. Development and characterization of aluminum matrix composites reinforced with

carbonized coconut shell and silicon carbide particle for automobile piston application. *Global Scientific Journals*, 2018; 6 (8): 390 – 398.

15. Nwabufoh M. N. *Development and Characterization of Al-3.7%Cu-1.4%Mg Alloy/Periwinkle Ash (Turritella Communis) Particulate Composites*. MEng. Thesis. Ahmadu Bello University, Zaria, Nigeria, 2015; 80p.
16. Hassan, S. B. and Aigbodion, V. S. The study of the microstructure and interfacial reaction of Al-Cu Mg/bagasse ash particulate composite. *Journal of Alloy and Compounds*, 2010; *491*: 571–574.
17. Rajan, T. P. D., Pillai, R. M., Pai B.C., Satyanaryana, K.G. and Rohatgi P.K. Fabrication and characterization of Al-7Si-0.35Mg/fly ash metal matrix composites processed by different stir casting routes. *Composites Science and Technology*, 2007; 67: 3369 – 3377.
18. Boppana, S. B., Dayanand, S., Kumar, A., Kumar, V. and Aravinda, T. Synthesis and characterization of nano graphene and ZrO_2 reinforced AA6061 metal matrix composites. *Journal of Materials Resource Technology*, 2020; 9: 7354–7362.
19. Monikandan, V. V., Joseph, M. A. and Rajendrakumar, P. K. Dry sliding wear of aluminium matrix hybrid composites. *Resource-Efficient Technologies, Elsevier*, 2016; 12 (3): 12 – 24.
20. Gun, Y. L., Dharana, C.K.H. and Ritchie, R.O. A physically-based abrasive wear model for composite materials. *Wear*, 2002; 252: 322–331.
21. Saravanan, S. D. and Kumar, M. S. Effect of mechanical properties on rice husk ash reinforced aluminium alloy ($AlSi_{10}Mg$) matrix composites. *Proceedings of Engineering*, 2013; 64: 1505 – 1513.
21. Aigbodion, V.S. *The Development and Characterization of Al-Cu-Mg/bagasse Ash Particulate Composites.* PhD Thesis. Ahmadu Bello University, Zaria, Nigeria, 2010; 176p.